Available online at www.sciencedirect.com
SCIENCE DIRECT®
Journal of Organometallic Chemistry 690 (2005) 6041–6050
Journal of Organometallic Chemistry
www.elsevier.com/locate/jorganchem

Luminescent coordination polymers with extended Au(I)–Ag(I) interactions supported by a pyridyl-substituted NHC ligand

Vincent J. Catalano *, Anthony O. Etogo

Department of Chemistry, University of Nevada, Reno, NV 89557, United States

Received 10 June 2005; accepted 29 July 2005
Available online 15 September 2005

Abstract

Reaction of $[Ag(CH_3impy)_2]PF_6$, **1**, with Au(tht)Cl produces the monometallic Au(I)-species $[Au(CH_3impy)_2]PF_6$, **2**. Treatment of **2** with excess $AgBF_4$ in acetonitrile, benzonitrile or benzylnitrile produces the polymeric species $\{[AuAg(CH_3impy)_2(L)](BF_4)_2\}_n$, (L = CH_3CN,**3**; L = C_6H_5CN, **4**; L = $C_6H_5CH_2CN$, **5**) where the Au(I) centers remain bound to two carbene moieties while the Ag(I) centers are coordinated to two alternating pyridyl groups and a solvent molecule (L). Reaction of **2** with $AgNO_3$ in acetonitrile produces the zig-zag mixed-metal polymer $\{[AuAg(CH_3impy)_2(NO_3)]NO_3\}_n$, **6**, that contains a coordinated nitrate ion in place of the coordinated solvent species. All of these polymeric materials are dynamic in solution and dissociate into their respective monometallic components. Compounds **2**–**6** are intensely luminescent in the solid-state and in frozen solution. All of these complexes were characterized by ^1H, ^{13}C NMR, electronic absorption and emission spectroscopy and elemental analysis.

Keywords: Coordination Polymer; Luminescence; Aurophilic; Carbene; Crystal Structures

1. Introduction

Attractive interactions between closed-shell metals have received considerable attention in recent years [1]. Among the most well-studied are the aurophilic attractions found between d^{10} Au(I) centers [2]. To a lesser degree mixed-metal interactions involving Ag(I)–Au(I) centers termed argento-aurophilic have been reported in the literature [3]. These non-bonding interactions are sufficiently strong to overcome the anticipated Coloumbic repulsion between like-charged metals, and extensive networks of cationic complexes can be formed in the solid-state [4]. Short aurophilic Au(I)–Au(I) interactions are also achievable through aggregation of linear, two-coordinate gold monomers in the solid-state or by the incorporation of bridging ligands [5]. Several theories have been advanced to rationalize these interactions, prominent among which are dispersion forces and relativistic effects [6].

The role of the former as the primary attractive force in metallophilic interactions has only been recently clarified, [7] whereas the latter has been known to play a significant role in maintaining the aurophilic attraction between Au(I) centers for quite some time [2,8]. In the case of mixed-metal interactions, the dispersion forces are enhanced by the introduction of dipolar interactions between dissimilar metals, resulting in shorter metal–metal separations than their respective homometallic species [9].

The luminescence attributed to these metal–metal interactions makes complexes with such properties very attractive towards potential applications such as luminescent display devices [10] and luminescent sensors for volatile organic compounds (VOC)[1b,c,11]. Because of gold's strong affinity for phosphorus we and others have extensively used chelating phosphines in the past as supports for metallophilic interactions, [12,13] either by encapsulating closed-shell metal ions or atoms in metallocryptands,

* Corresponding author. Tel.: +1 775 784 1329; fax: +1 775 784 6804.
E-mail address: vjc@unr.edu (V.J. Catalano).

0022-328X/$ - see front matter © 2005 Elsevier B.V. All rights reserved.
doi:10.1016/j.jorganchem.2005.07.109

or by forming multinuclear molecules with discrete aurophilic Au(I)–Au(I) or argento-aurophilic Ag(I)–Au(I) interactions. More recently we [9] and others [14] have turned out attention to the now ubiquitous N-heterocyclic carbene ligands [15] as possible supports for maintaining d^{10}–d^{10} interactions.

Earlier, we reported [16] the formation of a chiral coordination polymer, using the NHC ligand precursor, 1,3-bis(2-pyridyl)-1H-imidazolium tetrafluoroborate [H-$(py)_2$im]BF_4 as a support for stabilizing a Ag(I)–Au(I) interaction. The simple reaction (Scheme 1) of the gold monomer, [Au$((py_2)im)_2$]BF_4 with $AgBF_4$ in acetonitrile at room temperature or under reflux affords the helical coordination polymer {[AuAg$(py_2im)_2(CH_3CN)$][$(BF_4)_2$]}$_n$ with extended and short metal–metal separations of 2.8–2.9 Å. In the solid-state this species is intensely luminescent; however, in solution this material dissociates into its monometallic components. One notable feature of this helical polymer is the uncoordinated pyridyl group in each py_2im unit of the $[AuAg(py_2im)_2]^{2+}$ coordination core. In order to assess if the dynamic behavior was a result of the silver exchanging between these two sets of pyridyl in solution, we have now extended this chemistry to the closely related, yet unsymmetrical, mono-pyridyl-substituted ligand, [HCH_3impy]PF_6.

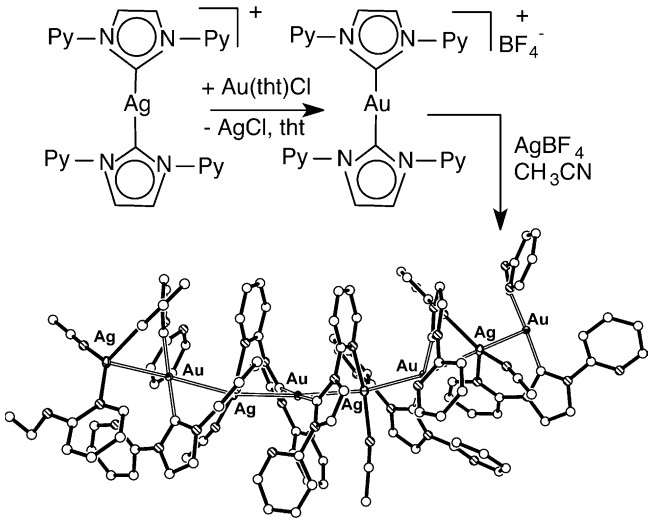

Scheme 1.

2. Results

As shown in Scheme 2, the imidazolium salt [HCH_3impy]PF_6, obtained by modifying a known procedure, [17] was deprotonated with Ag_2O in CH_2Cl_2, readily forming the homoleptic [Ag$(CH_3impy)_2$]PF_6 complex, **1**, in very good yield and purity. Metathesis to the analogous Au(I)-species [Au$(CH_3impy)_2$]PF_6, **2**, was accomplished using a simple carbene transfer reaction with Au(tht)Cl in either CH_2Cl_2 or CH_3CN. Further treatment of **2** with excess $AgBF_4$ in acetonitrile, benzonitrile and benzylnitrile coordinates a metal to the uncoordinated pyridyl moieties producing the polymeric species {[AuAg$(CH_3impy)_2$(L)]-$(BF_4)_2$}$_n$, (L = CH_3CN,**3**; L = C_6H_5CN, **4**; L = $C_6H_5CH_2$-CN, **5**). In these polymers the Au(I) centers remain bound to two carbene moieties while the Ag(I) centers are coordinated to two alternating pyridyl groups and a solvent molecule (L). Similarly, further treatment of **2** with $AgNO_3$ in acetonitrile results in the zig-zag mixed metal polymer {[AuAg$(CH_3impy)_2(NO_3)$]NO_3}$_n$, **6**, that contains a coordinated nitrate ion in place of the coordinated solvent species. The formation of **3**–**6** is independent of reaction temperature and stoichiometry; however, in solution these materials dissociate into their respective monomeric components (vide infra). Polymers **3**–**5** can be interconverted by dissolving the solids in the appropriate nitrile solvent and followed by precipitation with diethyl ether.

All of the aforementioned complexes were studied by ^{1}H NMR spectroscopy. In CD_3CN [H(CH_3impy)]PF_6 displays seven resonances, with the diagnostic singlet attributed to the proton on the carbene carbon appearing at 9.26 ppm. The remaining two protons on the backbone imidazole ring

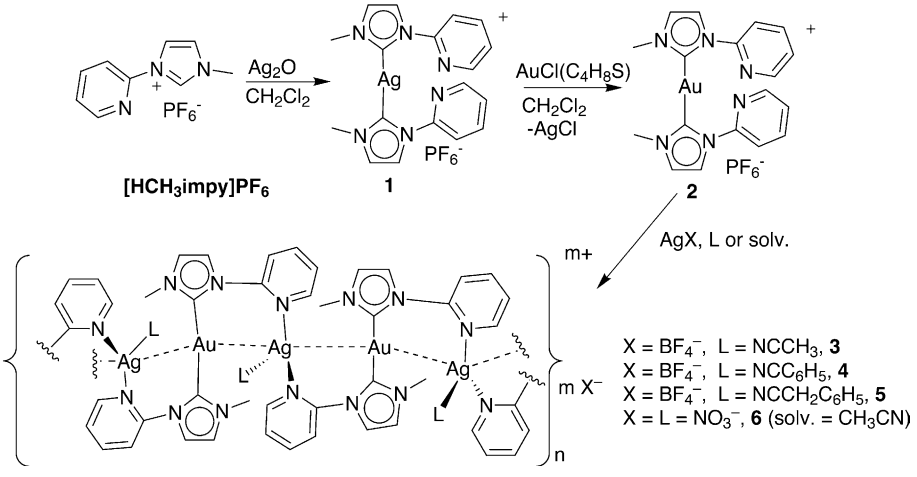

Scheme 2.

resonate at 8.06 and 7.55 ppm while the methyl resonance is observed at 3.96 ppm. Coordination to Ag(I) to form $[Ag(CH_3impy)_2]PF_6$, **1**, eliminates the downfield resonance and shifts the imidazole backbone resonances to 7.82 and 7.39 ppm. The methyl resonance, observed at 3.95 ppm is nearly unchanged. Replacing the Ag(I) for Au(I) to form $[Au(CH_3impy)_2]PF_6$ **2**, further shifts the imidazolium resonances to 7.76 and 7.48 ppm, but only minimally affects the methyl resonance which is now observed at 3.94 ppm. The room temperature solution spectra (CD_3CN) of **3**, **4**, **5**, and **6** are identical to that of **2** indicating that these polymers readily dissociate the silver ion in solution at room temperature leaving the pyridyl resonance unchanged relative to **2**. This exchange is facilitated by the presence of a donor solvent like CH_3CN, and unfortunately, none of these polymers are soluble enough in non-coordinating solvents to acquire a spectrum. Low temperature NMR experiments were equally disappointing, as the polymers precipitated out of solution as the temperature was reduced.

Complexes **1**–**6** were additionally characterized by single crystal X-ray diffraction. Crystallographic data are presented in Table 1. The colorless complex, $[Ag(CH_3impy)_2]PF_6$, **1**, crystallizes in the triclinic space group $P\bar{1}$, with one and one-half each of the cation and the hexafluorophosphate anion residing in the asymmetric unit. The remainder is related by a crystallographic center of inversion. The structure of the cationic portion containing Ag(1) is shown in Fig. 1 while selected bond distances and angles are tabulated in Table 2. Metrically, these two cations are nearly identical except for the relative orientations of the pyridyl rings and a small difference in the C–Ag–C angles. Each Ag(1) center is nearly linearly coordinated to two carbene ligands with C(10)–Ag(1)–C(1) and C(19)–Ag(2)–C(19)#1 angles of 173.09(16)° and 180.00 (19)°, respectively. The NHC ligands are oriented to opposite sides of the Ag(I) cation with the imidazole portions being nearly coplanar. The Ag(1)–C(1) and Ag(1)–C(10) separations measure 2.091(4) and 2.098(4) Å, respectively, while the corresponding Ag(2)–C(19) bond length is 2.090(4) Å. The Ag(1)···Ag(2) contact is long at 7.329 Å.

The analogous Au(I)-monomer $[Au(CH_3impy)_2]PF_6$, **2**, crystallizes in the monoclinic space group $P2_1/c$ with one-half of the cation and hexafluorophosphate counterion in the asymmetric unit each of which resides on a crystallographic inversion center. As displayed in Fig. 2 this symmetry makes the Au(I) center rigorously linear and the two imidazole rings coplanar. The Au(1)–C(1) separation of 2.0184(14) Å is slightly shorter the corresponding distance in **1**. Like **1** the two NHC ligands in **2** are oriented in a head-to-tail fashion with the pyridyl groups rotated about 38.8 ° relative to the NHC portion of the ligand. There are no short aurophilic contacts in **2**, and the shortest Au(I)···Au(I) separation is very long at 7.24 Å (see Table 3).

Addition of $AgBF_4$ to **2** in acetonitrile produces the mixed-metal, zig-zag polymer, $\{[AuAg(CH_3impy)_2(NCCH_3)](BF_4)_2\}_n$, **3**, shown in Figs. 3 and 7. This material

Table 1
Crystallographic data for complexes **1**–**2**

	1	**2**	**3** · CH_3CN	**4** · C_6H_5CN	**5** · 0.5 $C_6H_5CH_2CN$	**6**
Formula	$C_{27}H_{27}Ag_{1.50}F_9N_9P_{1.50}$	$C_{18}H_{18}AuF_6N_6P$	$C_{42}H_{45}Ag_2Au_2B_4F_{16}N_{15}$	$C_{32}H_{28}AgAuB_2F_8N_8$	$C_{30}H_{28.5}AgAuB_2F_8N_{7.50}$	$C_{36}H_{36}Ag_2Au_2N_{16}O_{12}$
F_w	856.84	662.34	1713.82	1003.08	969.03	1494.48
Crystal system	Triclinic	Monoclinic	Monoclinic	Monoclinic	Monoclinic	Monoclinic
Space group	$P\bar{1}$	$P2_1/c$	$P2_1/c$	$P2_1$	$P2_1/c$	$P2_1/n$
a (Å)	7.3106(5)	11.4499(8)	10.8203(8)	12.8475(10)	12.7675(6)	12.5732(6)
b (Å)	11.3541(8)	7.2472(5)	24.5537(19)	11.2028(9)	11.0228(5)	19.4854(9)
c (Å)	19.1956(14)	12.8951(9)	21.3513(17)	12.8387(10)	25.2070(12)	18.4598(9)
α (°)	98.4490(10)	90	90	90	90	90
β (°)	90.9200(10)	99.5840(10)	91.923(2)	96.010(2)	104.0470(10)	97.2840(10)
γ (°)	90.0430(10)	90	90	90	90	90
V (Å^3)	1575.83(19)	1055.10(13)	5669.4(8)	1837.6(3)	3441.4(3)	4486.0(4)
Z	2	2	4	2	4	4
Temperature (K)	100(2)	100(2)	100(2)	100(2)	100(2)	100(2)
R_1, wR_2 [$I > 2\sigma(I)$]	0.0431, 0.0984	0.0149, 0.0411	0.0466, 0.1138	0.0443, 0.1130	0.0484, 0.1330	0.0217, 0.0493

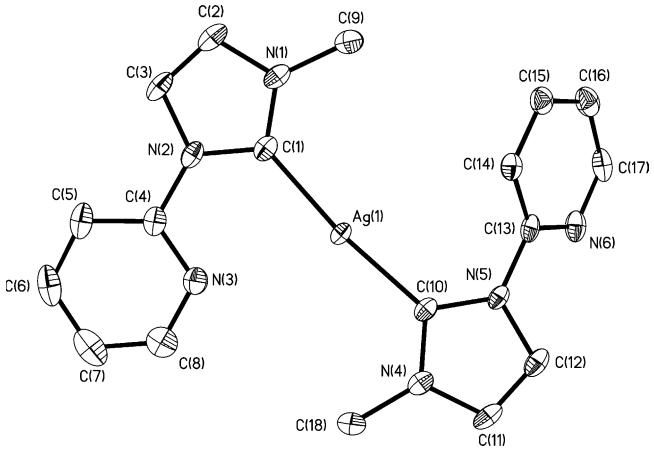

Fig. 1. X-ray structural drawing (50%) showing the cationic portion of $[Ag(CH_3impy)_2]PF_6$, **1**, with hydrogen atoms removed for clarity. Only the Ag(1) containing cation is shown.

Table 2
Selected bond distances (Å) and angles (deg) for $[Ag(CH_3impy)_2]PF_6$, **1**

Ag(1)–C(1)	2.091(4)
Ag(1)–C(10)	2.098(4)
Ag(2)–C(19)	2.090(4)
C(1)–N(1)	1.355(5)
C(1)–N(2)	1.368(5)
C(10)–N(4)	1.345(5)
C(10)–N(5)	1.370(5)
C(19)–N(7)	1.337(5)
C(19)–N(8)	1.367(5)
C(10)–Ag(1)–C(1)	173.09(19)
C(19)–Ag(2)–C(19A)	180
N(1)–C(1)–N(2)	104.1(3)
N(4)-C(10)-N(5)	103.7(3)
N(7)-C(19)-N(8)	104.2(3)
C(1)–N(2)–C(4)–N(3)	0.4(6)
C(10)–N(5)–C(13)–C(14)	41.4(6)
C(19)–N(8)–C(22)–C(23)	37.8(6)

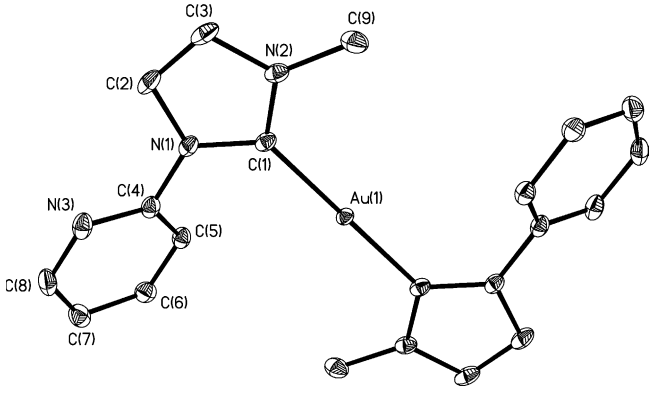

Fig. 2. Thermal ellipsoid drawing (50%) of cationic portion of $[Au(CH_3impy)_2]PF_6$, **2**, with hydrogen atoms removed for clarity. Only the crystallographically unique portion is labeled.

Table 3
Selected bond distances (Å) and angles (°) for $[Au(CH_3impy)_2]PF_6$, **2**

Au(1)–C(1)	2.0184(14)
C(1)–N(1)	1.3632(17)
C(1)–N(2)	1.3506(18)
N(1)–C(2)	1.3830(17)
N(2)–C(3)	1.3844(18)
C(2)–C(3)	1.345(2)
C(1)–Au(1)–C(1A)	180.0
N(1)–C(1)–N(2)	104.37(11)
Au(1)–C(1)–N(1)	128.87(10)
Au(1)–C(1)–N(2)	126.71(10)
C(1)–N(1)–C(4)–C(5)	41.7(2)

crystallizes in the monoclinic space group $P2_1/c$ with the asymmetric unit containing four metal atoms, four tetrafluoroborate anions and one acetonitrile solvate. Selected bond distances and angles are presented in Table 4. The d^{10}–d^{10} metal–metal separations are short with Au(1)–Ag(1), Ag(1)–Au(2) and Au(2)–Ag(2) separations of 2.9239(6), 2.8912(6), and 2.8633(6) Å, respectively. This metallo-chain repeats into the next symmetric unit with an Ag(2)–Au(1A) separation of 2.8873(6) Å. Three of the four intermetallic angles deviate significantly from linearity with Au(1)–Ag(1)–Au(2) and Ag(1)–Au(2)–Ag(2) measuring 175.37(3)° and 144.06(2)°, respectively, while the Au(2)–Ag(2)–Au(1A) and Ag(1)–Au(1)–Ag(2A) measure 166.85(2) and 135.20(2)° each. Each Au(I) center is coordinated to two NHC ligands in a nearly linear fashion with typical separations (Au(1)–C(1) = 2.017(7), Au(1)–C(28) = 2.013(7), Au(2)–C(10) = 2.015(8), and Au(2)–C(19) =2.007(7) Å) while each Ag(I) center is three-coordinated with two pyridyl moieties and one-coordinated solvent molecule. Because of ring strain imposed by the 6-membered dimetallacycle, the Ag–pyridyl separation are slightly longer than the Ag–acetonitrile separation. The Ag(1)–N(3) and Ag(1)–N(6) distances measure 2.306(6)

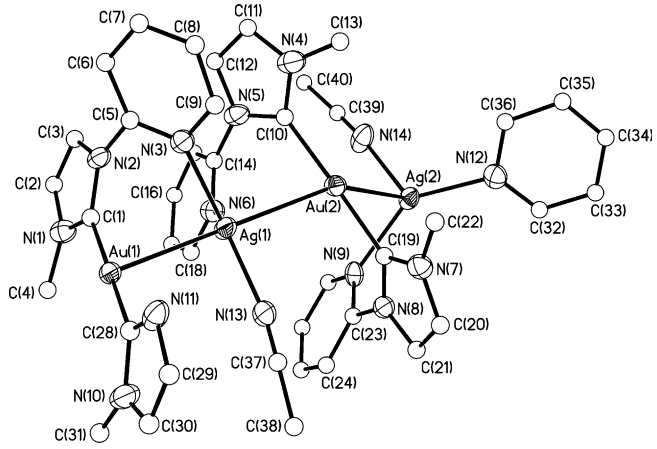

Fig. 3. X-ray structural drawing (40%) of the cationic portion of $\{[AuAg(CH_3impy)_2(NCCH_3)](BF_4)_2\}_n$, **3**, with carbon atoms drawn as circles and hydrogen atoms removed for clarity. Only the asymmetric unit is displayed. The extended polymer structure is presented in Fig. 7.

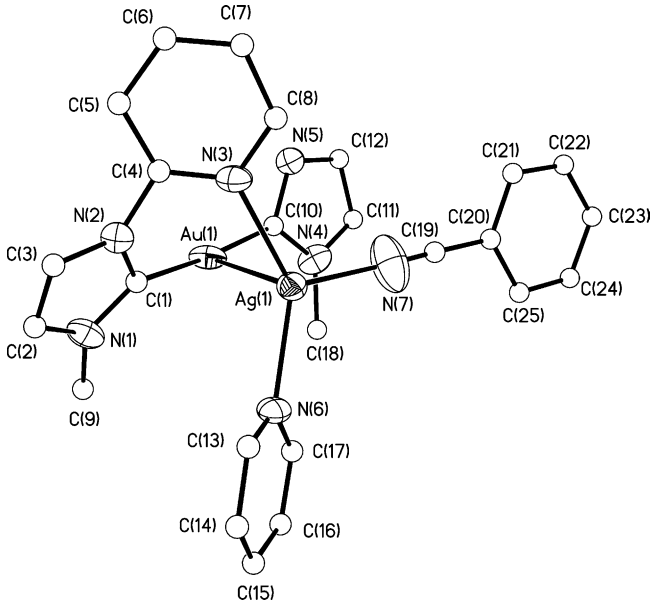

Fig. 4. X-ray structural drawing (40%) of the cationic portion of $\{[AuAg(CH_3impy)_2(NCC_6H_5)](BF_4)_2\}_n$, **4**, with carbon atoms drawn as circles and hydrogen atoms removed for clarity. Only the asymmetric unit is displayed. The extended polymer structure is presented in Fig. 7.

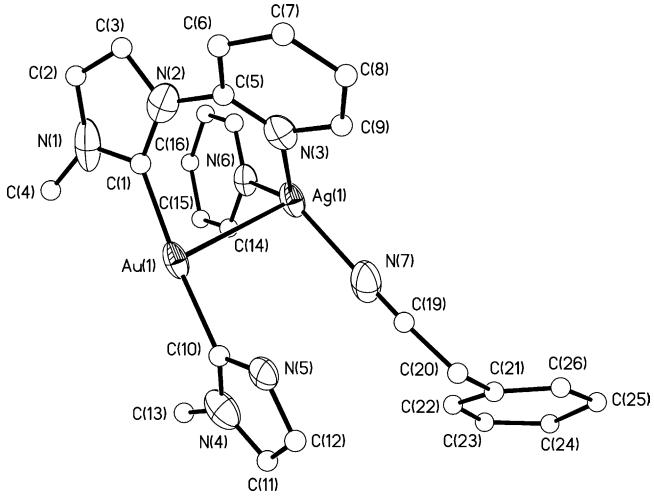

Fig. 5. X-ray structural drawing (40%) of the cationic portion of $\{[AuAg(CH_3impy)_2(NCCH_2C_6H_5)](BF_4)_2\}_n$, **5**, with carbon atoms drawn as circles and hydrogen atoms removed for clarity. Only the asymmetric unit is displayed. The extended polymer structure is presented in Fig. 7.

and 2.376(7) Å while the Ag(1)–N(13) is shorter at 2.193(7) Å. Likewise, the Ag(2)–N(9) and Ag(2)–N(12) separations are 2.304(6) and 2.245(7) Å, respectively, and the Ag(2)–N(14) bond distance is shorter at 2.238(7) Å. The metal–ligand angles around Ag(1) and Ag(2) range from 100.7(2)° to 138.3(2)° but sum to 359.9° and 359.5°, respectively indicating a planar environment.

Replacing the acetonitrile solvent with benzonitrile produces a similar polymer $\{[AuAg(CH_3impy)_2(NCC_6H_5)](BF_4)_2\}_n$, **4**, whose structure is depicted in Figs. 4 and 7. Selected bond distances and angles are shown in Table 5. Unlike **3** this material crystallizes in the chiral space group

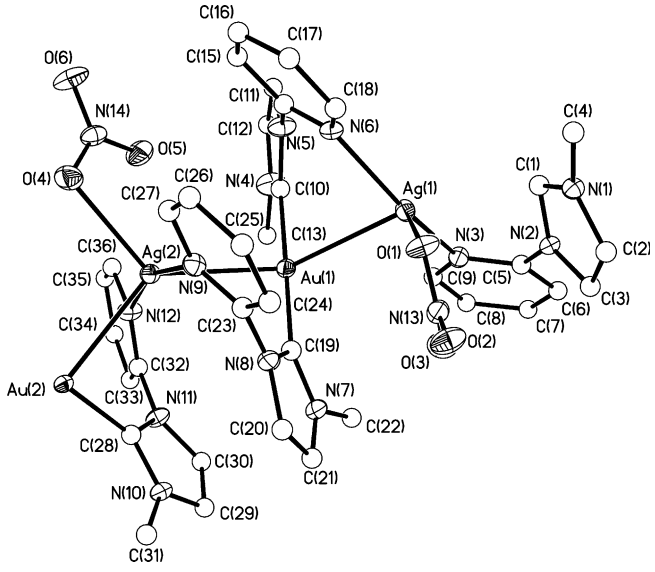

Fig. 6. X-ray structural drawing (50%) of the cationic portion of $\{[AuAg(CH_3impy)_2(NO_3)]NO_3\}_n$, **6**, with carbon atoms drawn as circles and hydrogen atoms removed for clarity. Only the asymmetric unit is displayed. The extended polymer structure is presented in Fig. 7.

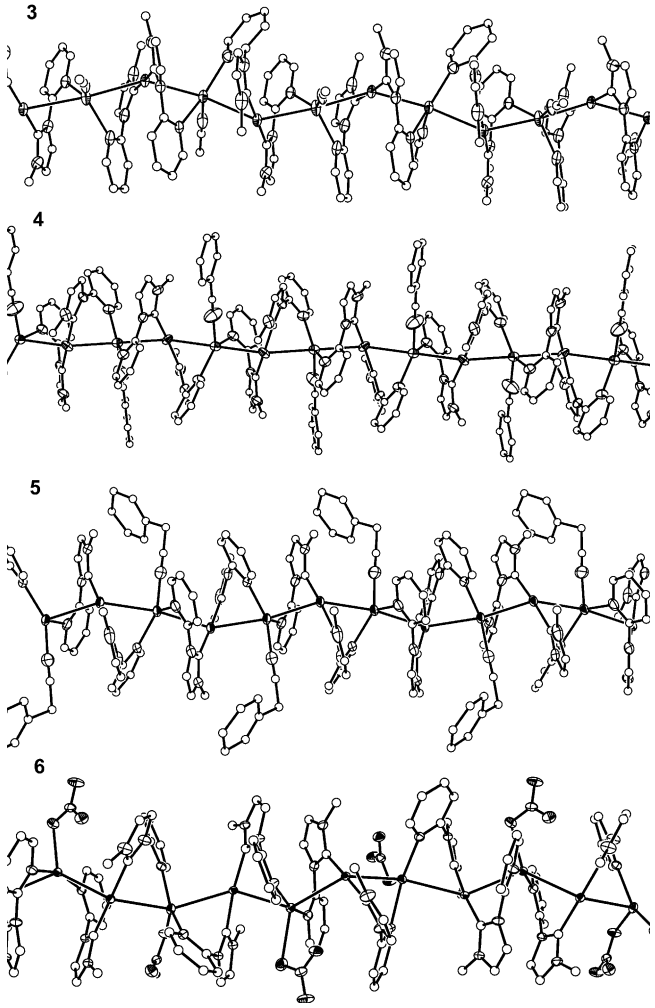

Fig. 7. Crystal structure drawing of the extended polymeric chains of **3** (*top*)–**6** (*bottom*) with carbon atoms drawn as circles and hydrogen atoms removed for clarity.

Table 4
Selected bond distances (Å) and angles (°) for $\{[AuAg(CH_3impy)_2(NCCH_3)](BF_4)_2\}_n$, **3**

Au(1)–Ag(1)	2.9239(6)
Ag(1)–Au(2)	2.8912(6)
Au(2)–Ag(2)	2.8633(6)
Au(1)–Ag(2A)	2.8873(6)
Au(1)–C(1)	2.017(7)
Au(1)–C(28)	2.013(7)
Au(2)–C(10)	2.015(8)
Au(2)–C(19)	2.007(7)
Ag(1)–N(3)	2.306(6)
Ag(1)–N(6)	2.376(7)
Ag(1)–N(13)	2.193(7)
Ag(2)–N(9)	2.304(6)
Ag(2)–N(12)	2.245(7)
Ag(2)–N(14)	2.238(7)
C(1)–Au(1)–Ag(1)–N(3)	66.6(3)
N(6)–Ag(1)–Au(2)–C(10)	62.8(3)
C(19)–Au(2)–Ag(2)–N(9)	66.8(3)
C(1)–N(2)–C(5)–N(3)	44.1(9)
C(10)–N(5)–C(14)–N(6)	40.0(10)
C(19)–N(8)–C(23)–N(9)	41.4(10)
Au(1)–Ag(1)–Au(2)–Ag(2)	145.9(3)
Au(1)–Ag(1)–Au(2)	175.37(3)
Ag(1)–Au(2)–Ag(2)	144.06(3)
Au(2)–Ag(2)–Au(1A)	166.85(2)
Ag(2A)–Au(1)–Ag(1)	135.20(2)
C(1)–Au(1)–C(28)	178.03(3)
C(10)–Au(2)–C(19)	176.6(3)
N(3)–Ag(1)–N(6)	100.7(2)
N(3)–Ag(1)–N(13)	121.8(2)
N(6)–Ag(1)–N(13)	137.4(2)
N(9)–Ag(2)–N(12)	138.3(2)
N(9)–Ag(2)–N(14)	102.1(3)
N(12)–Ag(2)–N(14)	119.1(3)
C(1)–Au(1)–Ag(1)	74.0(2)
C(28)–Au(1)–Ag(1)	106.7(2)
N(3)–Ag(1)–Au(2)	101.99(15)
N(6)–Ag(1)–Au(2)	74.32(16)
N(13)–Ag(1)–Au(2)	93.28(16)
C(10)–Au(2)–Ag(2)	109.5(2)
C(19)–Au(2)–Ag(2)	73.84(19)
N(9)–Ag(2)–Au(2)	77.15(14)
N(12)–Ag(2)–Au(2)	106.05(17)
N(14)–Ag(2)–Au(2)	91.42(18)

$P2_1$ with the cationic potion containing only a dimetallic repeating unit, two tetrafluoroborate anions and a benzonitrile solvent of crystallization. Although this crystal is chiral the bulk material is racemic and contains a statistical mixture of chiral crystals. The Au(1)–Ag(1) separation at 2.835(1) Å is slightly shorter than the corresponding separation in **3**. This chain is connected to the next with a Au–Ag separations of 2.833(1) Å. The angles between these metals are more regular than those in **3** with alternating Ag(1A)–Au(1)–Ag(1) and Au(1)–Ag(1)–Au(1A) angles of 162.429(8)° and 179.86(4)°, respectively. The Au(I) center is nearly linear with the C(1)–Au(1)–C(10) angle of 174.3(3)° and Au(1)–C(1) and Au(1)–C(10) separations of 2.011(8) and 2.021(8) Å, respectively. The Ag(I) center maintains a nearly trigonal planar environment with N(3)–Ag(1)–N(6), N(3)–Ag(1)–N(7), and N(6)–Ag(1)–N(7) angles of 137.1(2)°, 112.0(2)° and 110.9(5)°. The Ag–N separations are more regular with Ag(1)–N(3), Ag(1)–N(6), and Ag(1)–N(7) distances of 2.265(7), 2.268(7), and 2.273(10) Å respectively with very little difference between the separations of the coordinated benzonitrile and the pyridyl groups. The C(19)–N(7) separation at 1.105(13) Å is typical of a triple bond and is linearly coordinated to the Ag(1) center with a Ag(1)–N(7)–C(19) angle of 178.7(14)°.

Table 5
Selected bond distances (Å) and angles (°) for $\{[AuAg(CH_3impy)_2(NCC_6H_5)](BF_4)_2\}_n$, **4**

Au(1)–Ag(1)	2.835(1)
Ag(1)–Au(1A)	2.833(1)
Au(1)–C(1)	2.011(8)
Au(1)–C(10)	2.021(8)
Ag(1)–N(3)	2.265(7)
Ag(1)–N(6)	2.268((7)
Ag(1)–N(7)	2.273(10)
C(1)–Au(1)–Ag(1)–N(3)	67.7(3)
C(1)–N(2)–C(4)–N(3)	48.1(10)
Ag(1A)–Au(1)–Ag(1)	162.429(8)
Au(1)–Ag(1)–Au(1A)	179.86(4)
C(1)–Au(1)–C(10)	174.3(3)
N(3)–Ag(1)–N(6)	137.1(2)
N(3)–Ag(1)–N(7)	112.0(4)
N(6)–Ag(1)–N(7)	110.9(5)
C(1)–Au(1)–Ag(1)	73.6(3)
C(10)–Au(1)–Ag(1)	105.3(2)
N(3)–Ag(1)–Au(1)	78.83(18)
N(6)–Ag(1)–Au(1)	101.22(19)
N(7)–Ag(1)–Au(1)	90.0(3)

The benzylnitrile adduct only minimally perturbs the polymeric structure relative to **4**. The coordination polymer $\{[AuAg(CH_3impy)_2(NCCH_2C_6H_5)](BF_4)_2\}_n$, **5**, crystallizes in the centrosymmetric space group $P2_1/c$ with one repeating Ag–Au unit, two tetrafluoroborate anions and one-half of a benzylnitrile in the asymmetric unit. A view of the cationic portion is shown in Fig. 5 while selected bond distances and angles are presented in Table 6. The structural representation of the extended polymer chain is presented in Fig. 7. The Au(1)–Ag(1) separation is short at 2.8448(5) Å and connects to the next repeating unit with a separation of 2.8940(5) Å. This chain zig-zags with Ag(1)–Au(1)–Ag(1A) and Au(1)–Ag(1)–Au(1A) angles of 148.919(9)° and 170.87(2)° respectively. The NHC ligands are nearly linearly coordinated to Au(1) with a C(1)–Au(1)–C(10) angle of 174.7(3)° and Au(1)–C(1) and Au(1)–C(10) separations of 2.014(9) and 2.038(8) Å respectively. Similar to **3** the nitrile moiety is more tightly bound than the pyridyl groups. The Ag(1)–N(3) and Ag(1)–N(6) separations measure 2.327(6) and 2.283(5) Å while the Ag(1)–N(7) separation is shorter at 2.226(9) Å. These groups are arranged around Ag(1) in a trigonal planar fashion with N(3)–Ag(1)–N(6), N(3)–Ag(1)–N(7), and N(6)–Ag(1)–N(7) angles of 126.3(2)°, 108.0(3)° and 125.5(3)° respectively. The benzylnitrile group protrudes away from the metallic core and fills the void between

Table 6
Selected bond distances (Å) and angles (°) for $\{[AuAg(CH_3impy)_2(NCCH_2C_6H_5)](BF_4)_2\}_n$, **5**

Au(1)–Ag(1)	2.8448(5)
Au(1)–Ag(1A)	2.8940(5)
Au(1)–C(1)	2.014(9)
Au(1)–C(10)	2.038(8)
Ag(1)–N(3)	2.327(6)
Ag(1)–N(6)	2.283(5)
Ag(1)–N(7)	2.226(9)
N(7)–C(19)	1.124(13)
C(1)–N(2)–C(5)–N(3)	42.0(9)
C(1)–Au(1)–Ag(1)–N(3)	61.5(3)
Ag(1)–Au(1)–Ag(1A)	148.919(2)
Au(1)–Ag(1)–Au(1A)	170.87(2)
C(1)–Au(1)–C(10)	174.7(3)
N(3)–Ag(1)–N(6)	126.3(2)
N(3)–Ag(1)–N(7)	108.0(3)
N(6)–Ag(1)–N(7)	125.5(3)
Ag(1)–N(7)–C(19)	174.9(12)
N(7)–C(19)–C(20)	176.7(18)
C(19)–C(20)–C(21)	114.6(12)
C(1)–Au(1)–Ag(1)	80.1(2)
C(10)–Au(1)–Ag(1)	97.08(19)
N(3)–Ag(1)–Au(1)	76.59(14)
N(6)–Ag(1)–Au(1)	97.77(13)
N(7)–Ag(1)–Au(1)	97.86(19)

the polymer chains. The nitrile group is linear with a N(7)–C(19)–C(20) angle of 176.7(18)° and a N(7)–C(19) separation of 1.124(13) Å.

In an attempt to turn off the dynamic behavior of these polymers in solution, the coordinated nitriles were replaced with a coordinating nitrate anion. Accordingly, the colorless mixed-metal polymer $\{[AuAg(CH_3impy)_2(NO_3)]\text{-}NO_3\}_n$, **6**, readily crystallizes in the $P2_1/n$ space group with a repeating four-metal zig-zag chain bridged by NHC ligands, one-coordinated nitrate anion and one uncoordinated nitrate anion. Views of the cationic portion of **6** are presented in Figs. 6 and 7 while selected bond distances and angles are tabulated in Table 7. The metal–metal separations in **6** are similar to the other coordination polymers with Ag(1)–Au(1), Au(1)–Ag(2), and Ag(2)–Au(2) separations of 2.8125(2), 2.8460(2) and 2.8397(2) Å, and these chains are connected to each other with Ag–Au separations of 2.9428(2) Å. The angles between these metals are more acute than those in the other polymers with Au(1)–Ag(2)–Au(2) and Ag(1)–Au(1)–Ag(2) angles of 131.321(8) and 140.915(7)°. In between the chains angles of 146.883(9) and 143.053(7)° are observed for Au(1)–Ag(1)–Au(2A) and Ag(2)–Au(2)–Ag(1A) respectively. Each Au(I) center is linearly bound to the NHC ligands with Au(1)–C(10), Au(1)–C(19), Au(2)–C(1A) and Au(2)–C(28) distances of 2.012(3), 2.010(3), 2.022(2) and 2.022(3) Å respectively. The corresponding angles are close to linear with C(10)–Au(1)–C(19) and C(28)–Au(2)–C(1A) angles of 177.74(11)° and 173.39(10)° each. Coordination of the nitrate anions distorts the environment around the silver centers. The Ag(1)–O(1) and Ag(2)–O(4) separations are long at 2.451(2) and 2.564(2) Å while the Ag(1)–N(3),

Table 7
Selected bond distances (Å) and angles (°) for $\{[AuAg(CH_3impy)_2(NO_3)]\text{-}NO_3\}_n$, **6**

Ag(1)–Au(1)	2.8125(2)
Au(1)–Ag(2)	2.8460(2)
Ag(2)–Au(2)	2.8397(2)
Au(2)–Ag(1A)	2.9428(2)
Au(1)–C(10)	2.012(3)
Au(1)–C(19)	2.010(3)
Au(2)–C(28)	2.022(3)
Au(2)–C(1A)	2.022(2)
Ag(1)–O(1)	2.451(2)
Ag(1)–N(3)	2.273(2)
Ag(1)–N(6)	2.290(2)
Ag(2)–O(4)	2.564(2)
Ag(2)–N(9)	2.302(2)
Ag(2)–N(12)	2.297(2)
Ag(1)–O(1)	2.451(2)
Ag(1)–O(3)	3.093(3)
Ag(2)–O(5)	2.696(2)
Ag(1)–Au(1)–Ag(2)	140.915(7)
Au(1)–Ag(2)–Au(2)	131.321(8)
Au(1)–Ag(1)–Au(2A)	146.883(9)
Ag(2)–Au(2)–Ag(1A)	143.053(7)
C(10)–Au(1)–C(19)	177.74(11)
C(28)–Au(2)–C(1A)	173.39(10)
N(3)–Ag(1)–N(6)	150.21(8)
N(3)–Ag(1)–O(1)	121.50(8)
N(6)–Ag(1)–O(1)	88.24(8)
N(9)–Ag(2)–N(12)	161.43(8)
N(9)–Ag(2)–O(4)	87.50(8)
N(12)–Ag(2)–O(4)	110.64(8)
C(1)–N(2)–C(5)–N(3)	49.5(4)
C(10)–N(5)–C(14)–N(6)	52.0(4)
C(28)–N(11)–C(32)–N(12)	47.8(4)
Ag(1)–Au(1)–Ag(2)–Au(2)	120.006(12)

Ag(1)–N(6), Ag(2)–N(9) and Ag(2)–N(12) distances measure 2.273(2), 2.290(2), 2.302(2), and 2.297(2) Å respectively. The angles around each Ag ion deviate from the other coordination polymers with N(3)–Ag(1)–N(6), N(3)–Ag(1)–O(1), and N(6)–Ag(1)–O(1) angles of 150.21(8)°, 121.50(8)° and 88.24(8)° respectively. Similarly, the corresponding angles around the second silver center, N(9)–Ag(2)–N(12), N(9)–Ag(2)–O(4), and N(12)–Ag(2)–O(4), measure 161.43(8), 87.50(8) and 110.64(8)° each. Also noteworthy in **6** are the relatively large torsion angles between the imidazole and pyridyl groups. The C(1)–N(2)–C(5)–N(3), C(10)–N(5)–C(14)–N(6), and C(28)–N(11)–C(32)–N(12) angles at 49.5(4)°, 52.0(4)°, and 47.8(4)° are nearly 10° larger than the corresponding angles in **3**–**5**.

The electronic absorption spectra of **1** and **2** are nearly identical to that of $[HCH_3impy]PF_6$ with π–π* bands between 260 and 270 nm. Because the polymeric complexes dissociate into their respective monomers, in solution the electronic absorption spectra of **3** to **6** are nearly identical to **2**. All of the polymers are noticeably photoluminescent when excited with a hand-held UV lamp ($\lambda_x = 336$ nm). Both solutions and solid-state samples of the carbene precursor are photo-luminescent with a band appearing at 435 nm. Likewise, excitation of a solid samples of the monometallic Au containing species, **2**, produces a broad

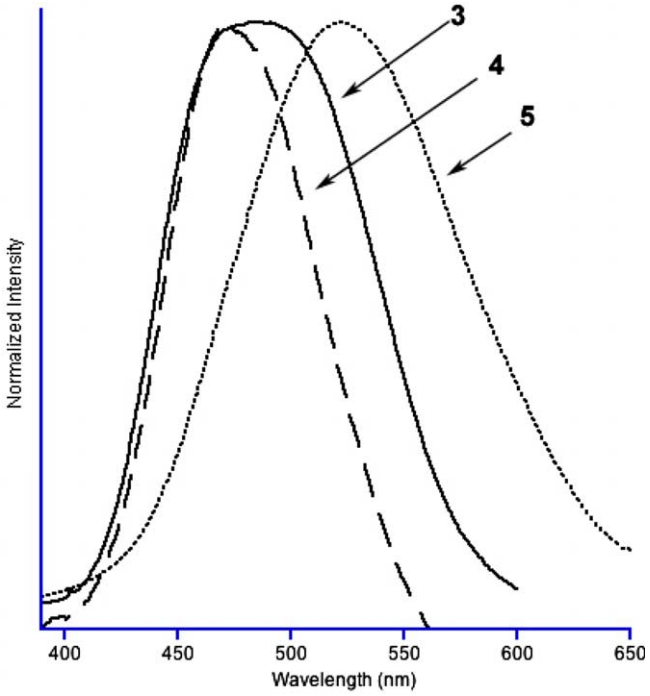

Fig. 8. Room temperature emission spectra of solid samples of the nitrile containing polymers **3**–**5**. The nitrate containing polymer has a spectrum nearly identical to that of **4**.

band at 541 nm ($\lambda_{ex} = 348$ nm). Cooling the solid to 77 K blue shifts this broad band to an emission maximum of 506 ($\lambda_{ex} = 340$ nm). At room temperature the solid-state emission spectra (Fig. 8) of the nitrile containing polymers show intense bands at 480, 474 and 522 nm ($\lambda_{ex} = 360$ nm) for the acetonitrile, benzonitrile and benzylnitrile containing polymers (**3**–**5**) respectively. The nitrate containing polymer **6** similarly has band that appears at 469 nm ($\lambda_{ex} = 383$). These spectra are independent of excitation wavelength. Cooling these solids to 77 K, sharpens and shifts these bands to 450, 480, 453 and 466 nm for **3**–**6**, respectively. Dissolving the polymers in acetonitrile disrupts the multimetallic framework, and emission spectra similar to that of **2** are observed. Freezing these solutions to 77 K produces intense emission bands around 500 nm similar to that of the $[Au(CH_3impy)_2]PF_6$, **2**, indicating that the polymer is no longer intact.

3. Discussion

The present study provides additional evidence for the versatility of N-heterocyclic carbenes as ligands in coordination chemistry, and as supports for d^{10} metallophilic interactions. It also further illustrates the generality of one-dimensional Au(I)–Ag(I) coordination polymer formation using the simple the pyridyl-imidazolium linkage of these NHC ligands. The propensity for polymer formation may be a consequence of the constrained Ag(I) coordination environment imposed by the rigid pyridyl-substituted carbene framework. In contrast, the insertion of a methylene spacer between the pyridyl group and the imidazole ring relieves this strain and only discrete dimetallic molecules are formed [18]. All the complexes reported are air stable, yet the polymers **3**–**6** readily dissociate Ag(I) ions in solution but reform the respective polymer chains upon precipitation. Replacement of the coordinated solvent molecule with a coordinating anion (nitrate in **6**) does not stop this dissociation. The loss of Ag(I) in solution is confirmed by the NMR spectroscopy which shows no change in four pyridyl resonances relative to **2**.

The observation of short Au–Ag separations is particularly interesting with both the shortest and longest Au(I)–Ag(I) separations of 2.8125(2) and 2.9482(2) Å found in the nitrate containing polymer, **6**. The changes in metal–metal separation within the different polymers, though subtle, demonstrates the significant impact of changing the coordinating solvent or anion on the basic structure of the polymer, and subsequently on its optoelectronic properties. This variation is even more striking considering the rigidity imposed by the constrained ligand backbone. While there are numerous reports in the literature on ligand-supported metal–metal interactions, [19] and clearly the strained scaffolding imposed by the rigid ligand backbone influences the short d^{10}–d^{10} interactions observed in **3**–**6**, recent reports have attributed shorter metal–metal interactions in mixed-metal species to an introduction of attractive dipolar interactions between the dissimilar metals [20]. For example, Fackler and coworkers [21] described the structures of three isomorphous $M_2(MTP)_2$ compounds where M_2 is Au_2, Ag_2 or AuAg and MTP is diphenylmethylenethiophosphinate and attributed the reduction in the mixed-metal separation (2.912 Å) relative to the homometallic separations (>3.0 Å) to an attractive dipolar interaction. Fernandez et al. [3a] also recently synthesized and structurally characterized the mixed Au(I)–Ag(I) ion pair complex, $[Ag(py)_3][Au(C_6F_5)_2]$, with an extended unsupported one-dimensional chain of alternating gold and silver atoms. According to their theoretical studies, the short Au(I)–Ag(I) interactions arise from both an attractive ionic(dipolar) contribution and from dispersion-type correlation effects. We recently reported the mixed-metal metallocryptands $[AuPdTl(P_2phen)_3](PF_6)_2$ and $[AuPtTl(P_2phen)_3](PF_6)_2$, where dipolar interactions shorten the M–Tl separations relative to those of their homometallic counterparts [22].

From a structural standpoint, the polymers **3**–**6** are particularly interesting. Although silver containing coordination polymers are well-known [23], **4** along with the previously reported $\{[AuAg((py)_2im)_2(CH_3CN)](BF_4)_2\}_n$ polymer are two rare examples of single-handed mixed-metal species derived from achiral ligands. Polymers **3**, **5** and **6** each contain helical one-dimensional multi-metallic chains but crystallize in a racemic fashion as dictated by their centrosymmetric space groups. Spontaneous resolution of racemic Ag-containing polymers from achiral components, although rare, has been reported elsewhere [24]. One of the more interesting features of the polymers reported here is

their differential luminescence. The origin of this difference is not well-understood. The trend of increasing energy of emission (**5** < **3** < **4**) does not correlate to decreasing Ag(I)–Au(I) separation or to the nitrile donor ability as measured by the nitrile–Ag separation. The origin likely resides in a combination of metal chain geometry and ancillary ligand electronic and steric properties. However, the significant changes in emission behavior reported here suggest that further substitution would lead to even more varied emission behavior. The photoluminescence of these materials and their potential applications [25] in optoelectronics and material science are also exciting avenues to explore in further detail in the near future.

4. Experimental

Solvents were used as received without purification or drying. The preparation of the imidazolium salt, [HCH_3impy]PF_6, was modified from a published procedure. [17] The preparation of Au(tht)Cl was described elsewhere [26]. UV–Vis spectra were obtained using a Hewlett–Packard 8453 diode array spectrometer (1 cm path-length cells). Emission data were recorded using a Spex Fluoromax steady-state fluorimeter.

4.1. Preparation of 1-methyl-3-(2-pyridinyl)-1H-Imidazolium hexafluorophosphate ([HCH_3impy]PF_6)

A mixture of 2-bromopyridine (3.8 mL, 40.0 mmol) and 1-methyl imidazole (3.2 mL, 40.0 mmol) was heated neat at 160 °C for 24 h. After cooling the resulting dark red oil was diluted with 30 mL of water, followed by addition of a saturated aqueous solution of 40.0 mmol NH_4PF_6. The precipitated solid was filtered and washed with two 30 mL portions of anhydrous Et_2O to afford 4.080 g (13.4 mmol) of 1-methyl-3-(2-pyridinyl)-1H-imidazolium hexafluorophosphate as an off white powder (33.4%). This material can be recrystallized from CH_3CN/Et_2O to afford a white powder. ^1H NMR (499.8 MHz, CD_3CN, 25 °C) $\delta = 9.25$ (s, 1H), 8.59 (m, 1H), 8.10 (m, 1H), 8.06 (m, 1H), 7.73 (d, 1H), 7.56 (m, 1H), 7.55 (d, 1H), 3.96 (s, 3H). ^{13}C $\{^1H\}$ NMR (125.7 MHz, CD_3CN, 25 °C) $\delta = 155.03$, 151.96, 146.04, 140.12, 130.92, 130.30, 124.76, 119.53, 42.01.

4.2. Preparation of [$Ag(CH_3impy)_2$]PF_6, 1

A 100 mL round bottom flask was charged with 0.107 g (0.35 mmol) of [HCH_3impy]PF_6 in 25 mL CH_2Cl_2, 0.020 g (0.088 mmol) Ag_2O, and a catalytic amount of Bu_4NPF_6. The mixture was protected from light and stirred for 1.5 hr at room temperature. NaOH (1 N, 3 mL) was then added, and stirring was continued for a further 15 min. The mixture was filtered through celite. The bright yellow filtrate was reduced to minimum volume under vacuum and precipitated with Et_2O affording 0.1700 g (0.27 mmol) of **2** as a white powder (75.3%). Anal. Calc. (%) ($C_{18}H_{18}N_6AgPF_6 \cdot H_2O$) C, 36.69; H, 3.42; N, 14.26. Found: C, 36.02; H, 3.25; N, 14.02. ^1H NMR (499.8 MHz, CD_3CN, 25 °C) $\delta = 8.36$ (m, 4.5 Hz, 2H), 7.93 (m, 8.5 Hz, 2H), 7.85(m, 2H), 7.82 (d, 2H), 7.42 (m, 2H), 7.93 (d, 2H), 3.95 (s, 6H). ^{13}C $\{^1H\}$ NMR (125.7 MHz, CD_3CN, 25 °C) $\delta = 150.50$, 147.86, 141.48, 135.58, 126.37, 125.74, 120.23, 114.99, 37.48. UV (CH_3CN) λ_{max}, nm (ε): 265 (33,300), 358 (2000), 487 (2000).

4.3. Preparation of [$Au(CH_3impy)_2$]PF_6, 2

A 50 ml round bottom flask was charged with 0.094 g (0.16 mmol) of **2** in 20 mL of CH_3CN. To this was added 0.052 g (0.16 mmol) of Au(tht)Cl dissolved in 10 mL of CH_3CN. The mixture was protected from light and stirred for 15 min after which solution was filtered through celite to remove the precipitated AgCl. The clear filtrate was reduced to minimum volume under vacuum and precipitated using Et_2O affording 0.098 g (0.10 mmol) of **2** as a white powder (90.0%). Anal. Calc. (%). ($C_{18}H_{18}N_6AuPF_6$) C, 32.74; H, 2.75; N, 12.73. Found: C, 32.42; H, 2.79; N, 12.62. ^1H NMR (499.8 MHz, CD_3CN, 25 °C) $\delta = 8.51$ (d, 4.5 Hz, 2H), 8.01 (d, 8.5 Hz, 2H), 7.88 (m, 8.5 Hz, 2H), 7.76 (d, 1.5 Hz, 2H), 7.48 (m, 4.5 Hz, 2H), 7.37 (d, 1.5 Hz, 2H), 3.94 (s, 6H). ^{13}C $\{^1H\}$ NMR (125.7 MHz, CD_3CN, 25 °C) $\delta = 183.57$, 151.67, 150.16, 140.34, 125.73, 125.43, 124.87, 121.98, 39.49. (CH_3CN) λ_{max}, nm (ε): 210 (22,000), 264 (16,000).

4.4. Preparation of {[$AuAg(CH_3impy)_2(NCCH_3)$]-$(BF_4)_2$}$_n$, 3

A 100 mL round bottom flask was charged with 0.071 g (0.10 mmol) of **3** and 0.021 g (0.13 mmol) of $AgBF_4$ in 30 mL CH_3CN. The colorless mixture was removed from light and stirred at room temperature for 1.5 h. The mixture was filtered through bulk celite, reduced to minimum volume under vacuum and precipitated with Et_2O affording 0.075g (0.04 mmol) of **3** as a white powder. (43.8%). Anal. Calc. (%) ($C_{20}H_{21}N_7AuAgB_2F_8$) C, 28.67; H, 2.52%; N, 11.70%. Found: C, 27.66; H, 2.19; N, 12.29.

4.5. Preparation of {[$AuAg(CH_3impy)_2(NCC_6H_5)$]-$(BF_4)_2$}$_n$, 4

Made analogously to **3** except benzonitrile is used in place of acetonitrile (57.7%). Anal. Calc. (%) ($C_{25}H_{23}N_7AuAgB_2F_8 \cdot 0.5\ C_6H_5CN$) C, 35.97; H, 2.70; N, 11.04. Found: C, 36.04; H, 2.42; N, 11.04.

4.6. Preparation of {[$AuAg(CH_3impy)_2(NCCH_2C_6H_5)$]-$(BF_4)_2$}$_n$, 5

Made analogously to **3** except benzylnitrile is used in place of acetonitrile (57.4%). Anal. Calc. (%) ($C_{26}H_{25}N_7AuAgB_2F_8 \cdot 0.5\ C_6H_5CH_2CN$) C, 37.05; H, 2.95; N, 10.80. Found: C, 36.64; H, 2.46; N, 10.8.

4.7. Preparation of $\{[AuAg(CH_3impy)_2(NO_3)]NO_3\}_n$, 6

Made analogously to **3** except $AgNO_3$ is used in place of $AgBF_4$ (58.8%). Anal. Calc. (%) ($C_{36}H_{36}N_{16}O_{12}Au_2Ag_2$) C, 28.93; H, 2.43; N, 14.99. Found: C, 29.30; H, 2.52; N, 14.65.

5. X-ray crystallography

Suitable crystals were coated in a hydrocarbon oil and mounted on a glass fiber. X-ray crystallographic data were collected at low temperature (100 K) using a Bruker SMART Apex CCD diffractometer with Mo Kα radiation and a detector-to-crystal distance of 4.94 cm. Data were collected in a full sphere using four set of frames with 0.3° scans in ω and an exposure time of 10s per frame. The 2θ range extended from 3.0 to 64°. Data were corrected for Lorentz and polarization effects using the SAINT program and corrected for absorption using SADABS or TWINABS. Unit cells were indexed using up to 9999 reflections harvested from the data collection. The structures were solved by direct methods and refined using the SHELXTL 5.12 software package [27].

6. Supporting information available

CCDC 273792–273797 contains the supplementary crystallographic data for this paper. These data can be obtained free of charge from The Cambridge Crystallographic Data Centre via www.ccdc.cam.ac.uk/data_request/cif.

Acknowledgment

This work and the X-ray diffractometer purchase were supported by the National Science Foundation (CHE-0091180 and CHE-0226402).

References

[1] (a) H. Schmidbaur, Nature 413 (2001) 31;
(b) M. Bardaji, A. Laguna, Eur. J. Inorg. Chem. (2003) 3061;
(c) E.J. Fernández, J.M. López-de-Luzuriaga, M. Monge, M.E. Olmos, J. Pérez, A. Laguna, A.A. Mohamed, J.P. Fackler Jr., J. Am. Chem. Soc. 125 (2003) 2022;
(d) E.J. Fernández, A. Laguna, J.M. López-de-Luzuriaga, M.E. Olmos, J. Pérez, Chem. Commun. (2003) 1760;
(e) V.W.-W. Yam, K.K.-W. Lo, Chem. Soc. Rev. 28 (1999) 323;
(f) L.H. Gade, Angew. Chem., Int. Ed. 40 (2001) 3573;
(g) E. Fernández, A. Laguna, J.M. López-de-Luzuriaga, Gold Bull. 34 (2001) 14.
[2] P. Pyykkö, Angew. Chem. Int. Ed. 43 (2004) 4412.
[3] (a) E.J. Fernández, A. Laguna, J.M. López-de-Luzuriaga, M. Monge, P. Pyykkö, N. Runeberg, Eur. J. Inorg. Chem. (2002) 750;
(b) V.J. Catalano, S.J. Horner, Inorg. Chem. 42 (2003) 8430;
(c) M.E. Olmos, A. Schier, H. Schmidbaur, Z. Naturforsch. B 52 (1997) 203.
[4] (a) R.L. White-Morris, M.M. Olmstead, A.L. Balch, O. Elbjeirami, M.A. Omary, Inorg. Chem. 42 (2003) 6741;
(b) A. Hamel, N.W. Mitzel, H. Schmidbaur, J. Am. Chem. Soc. 123 (2001) 5106;
(c) R.L. White-Morris, M.M. Olmstead, A.L. Balch, J. Am. Chem. Soc. 125 (2003) 1033.
[5] F.A. Cotton, B. Hong, Prog. Inorg. Chem. 40 (1992) 179.
[6] P. Pyykkö, M. Straka, Phys. Chem. Chem. Phys. 2 (2000) 2489.
[7] (a) F. Mendizabal, P. Pyykkö, A. Runeberg, Chem. Phys. Lett. 370 (2003) 733;
(b) N. Runeberg, M. Schütz, H.-J. Werner, J. Chem. Phys. 110 (1999) 7210.
[8] P. Pyykkö, F. Mendizabal, Chem. Eur. J. 3 (1997) 1458.
[9] V.J. Catalano, M.A. Malwitz, Inorg. Chem. 42 (2003) 548.
[10] (a) J.M. Forward, J.P. Fackler Jr., Z. Assefa, in: D.M. Roundhill, J.P. FacklerJr. (Eds.), Optoelectronic Properties of Inorganic Compounds, Plenum Press, New York, 1999, p. 195;
(b) Y. Ma, C.-M. Che, H.-Y. Chao, X. Zhou, W.-H. Chan, J. Shen, Adv. Mater. 11 (1999) 852.
[11] (a) C.E. Buss, K.R. Mann, J. Am. Chem. Soc. 124 (2002) 1031;
(b) M.A. Mansour, W.B. Connick, R.J. Lachicotte, H.J. Gysling, R. Eisenberg, J. Am. Chem. Soc. 120 (1998) 1329;
(c) L.G. Beauvais, M.P. Shores, J.R. Long, J. Am. Chem. Soc. 122 (2000) 2763;
(d) E. Cariati, X. Bu, P.C. Ford, Chem. Mater. 12 (2000) 3385.
[12] V.J. Catalano, B.L. Bennett, M.A. Malwitz, R.L. Yson, H.M. Kar, S. Muratidis, S.J. Horner, Comments Inorg. Chem. 24 (2003) 39.
[13] (a) R.J. Puddephatt, Coord. Chem. Rev. 216–217 (2001) 313;
(b) V.W.-W. Yam, K.K.-W. Lo, Chem. Soc. Rev. 28 (1999) 323.
[14] P.J. Barnard, M.V. Baker, S.J. Berners-Price, B.W. Skelton, A.H. White, Dalton Trans. 7 (2004) 1038.
[15] (a) T. Weskamp, V.P.W. Böhm, W.A. Herrmann, J. Organomet. Chem. 600 (2000) 12;
(b) W.A. Herrmann, T. Weskamp, V.P.W. Böhm, Adv. Organomet. Chem. 48 (2001) 1;
(c) I.J.B. Lin, C.S. Vasam, Comments Inorg. Chem. 25 (2004) 75;
(d) D. Bourissou, O. Guerret, F.P. Gabbaï, G. Bertrand, Chem. Rev. 100 (2000) 39;
(e) W.A. Herrmann, C. Köcher, Angew. Chem., Int. Ed. 36 (1997) 2162.
[16] V.J. Catalano, M.A. Malwitz, A.O. Etogo, Inorg. Chem. 43 (2004) 5714.
[17] S. Grünedemann, A. Kovacevic, M. Albrecht, J.W. Faller, R.H. Crabtree, J. Am. Chem. Soc. 124 (2002) 10473.
[18] V.J. Catalano, A.L. Moore, Inorg. Chem. 2005, in press.
[19] (a) J.S. MilerExtended Linear Chain Compounds, vols. 1–3, Plenum, New York, 1982;
(b) D.M. Roundhill, H.B. Gray, C.-M. Che, Acc. Chem. Res. 22 (1989) 55.
[20] (a) R. Usón, A. Laguna, M. Laguna, A. Usón, P.G. Jones, C.F. Erdbrügger, Organometallics 6 (1987) 1778;
(b) A. Usón, P.G. Jones, G.M. Sheldrick, J. Chem. Soc., Dalton Trans. (1984) 285.
[21] M.A. Rawashdeh-Omary, M.A. Omary, J.P. Fackler Jr., Inorg. Chim. Acta 334 (2002) 376.
[22] V.J. Catalano, M.A. Malwitz, J. Am. Chem. Soc. 126 (2004) 6560.
[23] A.N. Khlobystov, A.J. Blake, N.R. Champness, D.A. Lemenovskii, A.G. Majouga, N.V. Zyk, M. Schröder, Coord. Chem. Rev. 222 (2001) 155.
[24] (a) C. Janiak, T.G. Scharmann, P. Albrecht, F. Marlow, R. Macdonald, J. Am. Chem. Soc. 118 (1996) 6307;
(b) X.-H. Bu, W. Chen, M. Du, K. Biradha, W.-Z. Wang, R.-H. Zhang, Inorg. Chem. 41 (2002) 437;
(c) B.F. Abrahams, P.A. Jackson, R. Robson, Angew. Chem., Int. Ed. 37 (1998) 2656.
[25] C. Janiak, Dalton Trans. (2003) 2781.
[26] R. Usón, A. Laguna, M. Laguna, Inorg. Synth. 26 (1989) 85.
[27] XRD Single Crystal Software; Bruker Analytical X-ray Systems: Madison WI, 1999.